The Effect of Aperture Averaging Upon Tropospheric Delay Fluctuations Seen With a DSN Antenna

R. Linfield
Tracking Systems and Applications Section

The spectrum of tropospheric delay fluctuations expected for a DSN antenna at time scales <100 s has been calculated. A new feature included in these calculations is the effect of aperture averaging, which causes a reduction in delay fluctuations on time scales less than the antenna wind speed crossing time, ≈5–10 s. On time scales less than a few seconds, the Allan deviation $\sigma_y(\Delta t) \propto (\Delta t)^{+1}$, rather than $\sigma_y(\Delta t) \propto (\Delta t)^{-1/6}$ without aperture averaging. Due to thermal radiometer noise, calibration of tropospheric delay fluctuations with water vapor radiometers will not be possible on time scales less than ≈10 s. However, the tropospheric fluctuation level will be small enough that radio science measurements with a spacecraft on time scales less than a few seconds will be limited by the stability of frequency standards and/or other nontropospheric effects.

I. Introduction

Radio science experiments with a spacecraft use a one- or two-way radio link between a DSN antenna and the spacecraft. The received amplitude and phase are used to measure quantities such as gravitational radiation, refractivity profiles of the atmosphere of the planet or planetary satellite near the spacecraft, or the structure of a planetary ring system. Any perturbations on the link that are caused by the media between the DSN antenna and the spacecraft will corrupt the accuracy of the radio science measurement (unless the purpose of the experiment is to study that medium, e.g., the solar plasma). As the link frequency used for radio science experiments has increased, the relative magnitude of tropospheric and solar plasma phase fluctuations has changed dramatically, because plasma is dispersive at microwave frequencies and the troposphere is not. At S-band (2.3 GHz), solar plasma phase fluctuations dominate, while at Ka-band (32 GHz), tropospheric phase fluctuations will dominate except at small sun–spacecraft angular separations.

Knowledge of the tropospheric fluctuation spectrum will be useful in planning and analyzing radio science experiments. Comparison of fluctuation levels measured by very long baseline interferometry (VLBI) and water vapor radiometers (WVRs) has demonstrated that tropospheric delay/phase fluctuations at microwave frequencies are dominated by fluctuations in water vapor density [1].[1] The spectrum

[1] C. D. Edwards, "Water Vapor Radiometer Line-of-Sight Calibration Capabilities," JPL Interoffice Memorandum 335.1-90-015 (internal document), Jet Propulsion Laboratory, Pasadena, California, March 30, 1990.

of tropospheric fluctuations has been measured by VLBI on time scales >20 s [2] and by WVRs on time scales ≥200 s [3]. A model for these fluctuations has been developed [4]. Previous calculations using this model (e.g., [5]) have assumed a zero thickness "pencil beam" for a DSN antenna. However, on time scales less than ≈10 s, the nonzero diameter of a DSN antenna will modify this pencil beam spectrum. The method for calculating this "aperture averaging" effect is presented in Section II, and results are given in Section III. A short summary is given in Section IV.

II. Calculation of Aperture Averaging

Both theoretical arguments [6] and observational data [2,4,7] support the idea that tropospheric refractivity fluctuations obey a Kolmogorov power law. The refractivity structure function $D_n(r)$ on scales up to at least a few tens of kilometers is

$$D_n(r) \equiv \left\langle [N(\vec{x}+\vec{r}) - N(\vec{x})]^2 \right\rangle = C_n^2 r^{2/3} \tag{1}$$

where $N(\vec{x})$ is the refractivity at location $\vec{x}$ ($N \equiv n-1$, where n is the index of refraction), and C_n is the refractivity structure constant. Over time scales up to thousands of seconds, time variations in line-of-sight tropospheric delay can be successfully represented by a "frozen flow" model, in which spatial variations are convected past the observer by the wind.

The height dependence of C_n is poorly constrained by data. It was modeled by [4] as constant up to a 1-km height and zero above that. This "slab height" was subsequently revised to 2 km.[2] Recent WVR data from Goldstone [3] show that the observed fluctuations agree with the predictions of this 2-km slab model on time scales >400 s but are lower than model predictions on shorter time scales. This result is most easily explained by a thickness of the turbulent layer that is significantly larger than 2 km, although the data are not adequate to solve for a specific value for this thickness. The effect of a finite thickness h of the medium is that fluctuations in the vertical dimension saturate on time scales $> h/v_w$, where v_w is the wind speed. For time scales $\Delta t << h/v_w$, the delay structure function $D_\tau \propto (\Delta t)^{5/3}$, and for time scales $\Delta t >> h/v_w$, $D_\tau \propto (\Delta t)^{2/3}$ [4]. The time scales covered in this article are all $<< h/v_w$. WVR measurements of fluctuations on time scales of 200 s [3] were used to derive the mean C_n, once h was chosen. For $h = 4$ km, $C_n = 3.0 \times 10^{-8}$ m$^{-1/3}$; these values were used for all calculations presented in this article. Over the course of a year, the structure constant at Goldstone exhibits variations of at least a factor of 2 about its mean value [3].

The tropospheric delay for a pencil beam looking from location $\vec{x}$ at elevation angle θ and azimuth AZ is

$$\tau_{pencil}(\vec{x}, \theta, AZ) = \frac{1}{\sin\theta} \int_0^\infty N\left[\vec{x} + \vec{r}(\theta, AZ, z)\right] dz \tag{2}$$

where $\vec{r}(\theta, AZ, z)$ is the vector from the surface to height z in direction (θ, AZ). For a DSN antenna of diameter d, the delay is averaged over the circular aperture, to give

$$\tau_{DSN}(\vec{x}, \theta, AZ) = \frac{4}{\pi d^2} \int_0^{2\pi} \int_0^{d/2} \xi \tau_{pencil}\left[\vec{x} + \vec{r}(\xi, \phi), \theta, AZ\right] d\xi d\phi \tag{3}$$

where $\vec{r}(\xi, \phi)$ is the vector in the plane of the aperture, starting from the center, of length ξ and at angle ϕ (the direction chosen for $\phi = 0$ does not affect the result). Equation (3) assumes that the near-field

[2] R. N. Treuhaft, personal communication, Jet Propulsion Laboratory, Pasadena, California, 1995.

DSN beam profile is uniform across its circular cross section. The true profile will be tapered towards the edges. As presented in Section III, a change of a factor of two in antenna diameter causes a change in the resulting fluctuation level by a factor of ≈2. Therefore, neglect of beam tapering should cause an error of <20 percent in the results reported here.

A convenient way of calculating and expressing the tropospheric fluctuation spectrum is Allan variance $\sigma_y^2(\Delta t)$, defined for a delay process $\tau(t)$ as [8]

$$\sigma_y^2(\Delta t) \equiv \frac{\left\langle [\tau(t+2\Delta t) - 2\tau(t+\Delta t) + \tau(t)]^2 \right\rangle}{2\,(\Delta t)^2} \tag{4}$$

Expanding Eq. (4) and assuming that averaged quantities are independent of time and position gives, for the tropospheric delay fluctuations measured by a DSN antenna,

$$\sigma_y^2(\Delta t) = \frac{3\left\langle \tau_{DSN}^2(t) \right\rangle}{(\Delta t)^2} - \frac{4\left\langle \tau_{DSN}(t+\Delta t)\tau_{DSN}(t) \right\rangle}{(\Delta t)^2} + \frac{\left\langle \tau_{DSN}(t+2\Delta t)\tau_{DSN}(t) \right\rangle}{(\Delta t)^2} \tag{5}$$

We can evaluate this expression with Eq. (3) and the frozen-flow assumption. Taking the middle term in Eq. (5) as an example,

$$\left\langle \tau_{DSN}(t+\Delta t)\tau_{DSN}(t) \right\rangle = \frac{16}{\pi^2 d^4} \int_0^{2\pi} \int_0^{2\pi} \int_0^{d/2} \int_0^{d/2} \xi\xi' \left\langle \tau_{pencil}\left[\vec{x} + \vec{v}_w \Delta t + \vec{r}(\xi,\phi)\right] \tau_{pencil}\left[\vec{x} + \vec{r}(\xi',\phi')\right] \right\rangle$$

$$\times\, d\xi d\xi' d\phi d\phi'$$

It has been assumed that averaged quantities are position independent, so that

$$\left\langle \tau_{pencil}(\vec{x}_1,\theta,AZ)\tau_{pencil}(\vec{x}_2,\theta,AZ) \right\rangle = \left\langle \tau_{pencil}^2(\vec{x},\theta,AZ) \right\rangle - \frac{1}{2}\left\langle [\tau_{pencil}(\vec{x}_1,\theta,AZ) - \tau_{pencil}(\vec{x}_2,\theta,AZ)]^2 \right\rangle$$

$$= \left\langle \tau_{pencil}^2(\vec{x},\theta,AZ) \right\rangle - \frac{1}{2} D_\tau\left(|\vec{x}_1 - \vec{x}_2|\right)$$

where D_τ is the pencil-beam delay structure function, defined as

$$D_\tau(r) \equiv \left\langle [\tau_{pencil}(\vec{x}+\vec{r},\theta,AZ) - \tau_{pencil}(\vec{x},\theta,AZ)]^2 \right\rangle$$

In evaluating Eq. (5), the $\left\langle \tau_{pencil}^2(\vec{x}) \right\rangle$ terms add to zero, and $\sigma_y^2(\Delta t)$ can be expressed as a four-dimensional integral of three D_τ terms:

$$\left.\begin{aligned}\sigma_y^2(\Delta t) =& \frac{16}{\pi^2 d^4 (\Delta t)^2}\int_0^{2\pi} d\phi \int_0^{2\pi} d\phi' \int_0^{d/2} \xi d\xi \int_0^{d/2} \xi' d\xi \left[-\frac{3}{2}D_\tau(A) + 2D_\tau(B) - \frac{1}{2}D_\tau(C)\right] \\ A =& |\vec{r}(\xi,\phi) - \vec{r}(\xi',\phi')| \\ B =& |\vec{v}_w \Delta t + \vec{r}(\xi,\phi) - \vec{r}(\xi',\phi')| \\ C =& |2\vec{v}_w \Delta t + \vec{r}(\xi,\phi) - \vec{r}(\xi',\phi')|\end{aligned}\right\} \quad (6)$$

The horizontal distance scales are d and $v_w \Delta t$. As a result, $\sigma_y(\Delta t)$ will be suppressed, relative to its $d = 0$ value, for values of Δt smaller than a few times the wind speed crossing time of $t_{cross} = d/v_w$. For a typical wind speed in the lower few kilometers of 8 m/s and for $d = 34$ m, $t_{cross} \approx 5$ s. For $\Delta t << t_{cross}$, $\sigma_y(\Delta t)$ will be much lower than its $d = 0$ value, due to the averaging of many small-scale delay fluctuations over the much larger DSN aperture.

For any DSN tracking scenario at an observing frequency high enough ($\geq$8 GHz) for tropospheric delay fluctuations to dominate over those from plasma, the Earth's troposphere will lie entirely within the near field of the antenna. The effective tropospheric volume sampled by the DSN antenna will then be cylindrical. For tracking of planetary spacecraft, the antenna will move at a nearly sidereal rate. This tracking will cause an effective velocity v_{eff} through the troposphere, at height z and elevation angle θ, of

$$v_{eff} = \frac{\Omega z}{\sin\theta}$$

The Earth's rotation rate is Ω. For $z = 2$ km (half the turbulent slab height), $v_{eff} = 0.15/\sin\theta$ m/s. This is much less than the wind speed of 8 m/s used in the calculations. Sidereal tracking, therefore, will not significantly modify the results presented in this article.

The Fresnel length scale l for observations at a wavelength λ with phase perturbations occurring at a distance L is $l \approx \sqrt{\lambda L}$. For $\lambda = 1$ cm and $L = 2$ km (the middle of the turbulent troposphere), $l \approx 4$ m. On smaller scales, geometric optics is not completely valid. The results for time scales <4 m/s$/v_w = 0.5$ s should, therefore, be regarded as approximate.

III. Results

Equation (6) was evaluated numerically, for a range of time intervals, and for both 34-m- and 70-m-diameter antennas. A wind speed of 8 m/s was assumed. The results for antennas pointed in the zenith direction are shown in Fig. 1. Values of $\sigma_y(\Delta t)$ for a pencil beam antenna are shown for comparison.

For time intervals shorter than 10 s, the Allan deviation for measurements made with a DSN antenna are less than those made with a pencil beam. For time intervals less than $\approx$2 s, $\sigma_y(\Delta t) \propto (\Delta t)^k$, where $k \approx +1$. This proportionality can be roughly understood as follows: The effect of fluctuations over a time interval Δt are confined to a region of size $\approx v_w \Delta t$. For $v_w \Delta t << d$, there are $N_{regions} \sim (d/(v_w \Delta t))^2$ such regions over the antenna aperture. Averaging the delay fluctuations of these regions will cause a reduction by a factor of $\sim\sqrt{N_{regions}} \sim d/(v_w \Delta t)$. The slope of the pencil beam $\sigma_y(\Delta t)$ is $\approx -1/6$, so the slope of the DSN $\sigma_y(\Delta t)$ will be $\approx +5/6$.

As Δt decreases, the amount of computer time needed to calculate $\sigma_y(\Delta t)$ increases rapidly. For small Δt, the terms A, B, and C in Eq. (6) are nearly equal, and high numerical precision is needed in order

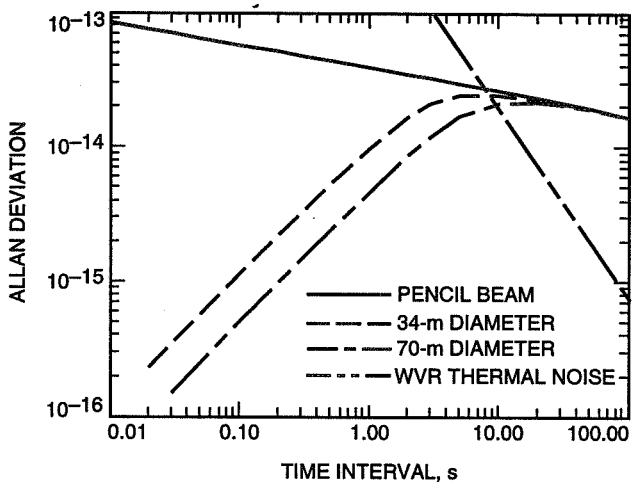

Fig. 1. The Allan deviation calculated for a pencil beam antenna and for antenna diameters of 34 and 70 m is shown as a function of time interval for typical Goldstone conditions and the zenith direction. The Allan deviation at other elevation angles will be somewhat larger, increasing by a factor of 1.8 at a 10-deg elevation angle. The thermal noise from a WVR with the characteristics expected for the Cassini radio science calibration system is included.

to determine the differences in the D_τ terms. Furthermore, all derivatives of D_n and all but the first derivative of D_τ become singular at zero separation, so that numerical integration methods have difficulty.

Calculations for Δt as small as 0.02 s were possible in the zenith direction, because $D_\tau(r)$ could be evaluated separately, with an empirically fitted analytical formula used for D_τ in Eq. (6) to reduce the number of dimensions in the integration from 6 to 4. Calculations at other elevation angles were limited to a narrower range of time intervals (1–100 s). These calculations showed that $\sigma_y(\Delta t)$ increases slowly with decreasing elevation angle. Relative to its value at the zenith, $\sigma_y(\Delta t)$ was 1.16 times larger at a 30-deg elevation angle and 1.82 times larger at a 10-deg elevation angle.

All $\sigma_y(\Delta t)$ values in Fig. 1 are linearly proportional to the structure constant, C_n. Therefore, the actual $\sigma_y(\Delta t)$ values at a DSN site will range up and down from those in Fig. 1 by a factor of at least 2, depending upon the season, time of day, and weather conditions. Winter nights tend to have the lowest C_n values, with summer days having the largest values.

Tropospheric delay fluctuations at microwave frequencies can be calibrated by WVRs, which measure thermal emission from water vapor in the vicinity of its 22-GHz spectral line [9]. However, on short time scales, the thermal noise from a WVR becomes the limiting error source. The main vapor-sensing channel of current WVRs is at a frequency near 21.5 or 23.8 GHz, where a 1-K brightness temperature corresponds to $\approx$6 mm/$c = 2 \times 10^{-11}$ s of path delay (c is the speed of light). The thermal path delay equivalent noise in a WVR measurement of integration time t_{int} for a total system temperature T_{sys} and bandwidth BW is

$$N(t_{int}) = \frac{T_{sys}}{\sqrt{BW\ t_{int}}} \cdot \frac{2 \times 10^{-11}\ \text{s}}{1\text{K}} = \frac{2 \times 10^{-13} T_{100}}{BW_{100}^{0.5}\ t_{int_s}^{0.5}}\ \text{s} \tag{7}$$

where $T_{100} \equiv T_{sys}/100$ K, $BW_{100} \equiv BW/100$ MHz, and $t_{int_s} \equiv t_{int}/1$ s.

To set a firm lower limit on the effect of WVR thermal noise, we assume that $\Delta t = t_{int}$ (i.e., we give up all information on time scales shorter than Δt). Future uncooled WVRs currently under design are expected to have $T_{sys} \approx 300$ K and $BW \approx 400$ MHz.[3] The Allan deviation from thermal WVR noise for $\Delta t_s = \Delta t/1$ s (note that $\sigma_y(\Delta t) = N(t_{int})\sqrt{3}/\Delta t$ for thermal noise) then is

$$\sigma_y(\Delta t) \approx \frac{5 \times 10^{-13}}{\Delta t_s^{1.5}} \quad \text{(WVR thermal noise)} \tag{8}$$

This WVR thermal noise curve is plotted in Fig. 1. If we require $\sigma_y(\Delta t)$ from WVR thermal noise to be at least 3 times smaller than the tropospheric $\sigma_y(\Delta t)$ in order to achieve useful calibration, then, for any elevation angle $\geq$10 deg, the minimum time interval Δt_{min} for WVR calibration is

$$\Delta t_{min} \approx 10 \text{ s}$$

Because the slope of the tropospheric $\sigma_y(\Delta t)$ is small at $\Delta t \sim 10$ s and the slope of the WVR thermal noise $\sigma_y(\Delta t)$ is steep, the minimum useful calibration interval is relatively insensitive to the values of T_{sys} and BW. On time scales less than $\approx$10 s, tropospheric fluctuations cannot be calibrated with any known technique.

IV. Summary

The effect of aperture averaging upon radio science measurements is that tropospheric fluctuations will not be important on short time scales. For occultation measurements of Saturn's rings with Cassini, the shortest time scale of interest is the desired physical resolution ($\approx$100 m) divided by the spacecraft orbital velocity ($\approx$10 km/s), or $\sim$0.01 s.[4] These measurements will use an onboard oscillator with $\sigma_y(\Delta t) \geq 10^{-13}$. Even if future flight oscillators were a factor of 10 more stable than the one on Cassini, the troposphere would be more stable than the oscillator for $\Delta t < 1$ s. The tropospheric fluctuations on $\Delta t < 10$ s appear to form a fundamental lower limit for radio science measurements using an Earth antenna, because WVR thermal noise precludes calibration of the fluctuations.

Acknowledgments

I thank J. Armstrong, G. Lanyi, and C. Naudet for helpful suggestions on writing this article.

References

[1] G. Elgered, J. L. Davis, T. A. Herring, and I. I. Shapiro, "Geodesy by Radio Interferometry: Water Vapor Radiometry for Estimation of the Wet Delay," *J. Geophy. Res.*, vol. 96, no. B4, pp. 6541–6555, 1991.

[3] A. B. Tanner, personal communication, Jet Propulsion Laboratory, Pasadena, California, November 27, 1995.

[4] N. Rappaport, personal communication, Jet Propulsion Laboratory, Pasadena, California, November 21, 1995.

[2] R. P. Linfield, S. J. Keihm, L. P. Teitelbaum, S. J. Walter, M. J. Mahoney, R. N. Treuhaft, and L. J. Skjerve, "A Test of Water Vapor Radiometer-Based Troposphere Calibration Using Very Long Baseline Interferometry Observations on a 21-km Baseline," *Radio Science*, 1996 (in press).

[3] S. J. Keihm, "Water Vapor Radiometer Measurements of the Tropospheric Delay Fluctuations at Goldstone Over a Full Year," *The Telecommunications and Data Acquisition Progress Report 42-122, April–June 1995*, Jet Propulsion Laboratory, Pasadena, California, pp. 1–11, August 15, 1995.

[4] R. N. Treuhaft and G. E. Lanyi, "The Effect of Dynamic Wet Troposphere on Radio Interferometric Measurements," *Radio Science*, vol. 22, no. 22, pp. 251–265, 1987.

[5] R. P. Linfield and J. Z. Wilcox, "Radio Metric Errors Due to Mismatch and Offset Between a DSN Antenna Beam and the Beam of a Troposphere Calibration Instrument," *The Telecommunications and Data Acquisition Progress Report 42-114, April–June 1993*, Jet Propulsion Laboratory, Pasadena, California, pp. 1–13, August 15, 1993.

[6] V. I. Tatarski, *Wave Propogation in a Turbulent Medium*, New York: Dover, 1961.

[7] A. E. E. Rogers, A. T. Moffet, D. C. Backer, and J. M. Moran, "Coherence Limits in VLBI Observations at 3-mm Wavelength," *Radio Science*, vol. 19, pp. 1552–1560, 1984.

[8] D. W. Allan, "Statistics of Atomic Frequency Standards," *Proc. IEEE*, vol. 54, no. 2, pp. 221–230, 1966.

[9] G. Elgered, "Tropospheric Radio Path Delay From Ground-Based Microwave Radiometry," Chapter 5, *Atmospheric Remote Sensing by Microwave Radiometry*, edited by M. Janssen, New York: Wiley & Sons, 1993.